

High-pressure Brillouin scattering of $\text{Pb}(\text{Mg}_{1/3}\text{Nb}_{2/3})\text{O}_3$

Muhtar Ahart,¹ Maddury Somayazulu,¹ Zuo-Guang Ye,² R. E. Cohen,¹
Ho-kwang Mao,¹ and Russell J. Hemley¹

¹*Geophysical Laboratory, Carnegie Institution of Washington, 5251 Broad Branch Rd., NW, Washington, DC 20015, USA*

²*Department of Chemistry and 4D LABS, Simon Fraser University, Burnaby, British Columbia, Canada V5A 1S6*

(Received 2 January 2009; revised manuscript received 24 February 2009; published 13 April 2009)

The pressure dependencies of the elastic constants and bulk modulus of single crystal $\text{Pb}(\text{Mg}_{1/3}\text{Nb}_{2/3})\text{O}_3$ (PMN) have been measured up to 10 GPa at room temperature by Brillouin spectroscopy. The elastic moduli and elastic anisotropy undergo an abrupt change at 4.5 GPa, indicative of a phase transition and consistent with earlier Raman and x-ray diffraction studies. We suggest that PMN undergoes a structural change from a cubic $Pm\bar{3}m$ to rhombohedral $R3c$ phase at 4.5 GPa.

DOI: 10.1103/PhysRevB.79.132103

PACS number(s): 77.90.+k, 77.65.-j, 78.35.+c

$\text{Pb}(\text{Mg}_{1/3}\text{Nb}_{2/3})\text{O}_3$ (PMN) is a prototypical relaxor and an end member of the relaxor ferroelectric solid solution $(1-x)\text{Pb}(\text{Mg}_{1/3}\text{Nb}_{2/3})\text{O}_3-x\text{PbTiO}_3$ (PMN- x PT). These materials have generated a great deal of interest due to their superior electromechanical properties¹ compared to the conventional $\text{PbZr}_x\text{Ti}_{(1-x)}\text{O}_3$ ceramics that have dominated piezoelectric applications for more than 40 years. While extensive theoretical and experimental studies¹⁻⁴ have greatly advanced our understanding of relaxors, many of the properties of relaxors still remain unclear.⁴ These difficulties stem from the complexity of these materials, which have a high degree of compositional and structural disorder.

PMN has the perovskite structure with cubic $m\bar{3}m$ macroscopic symmetry,⁵ with Mg^{2+} and Nb^{5+} ions disordered on the B sites. Measurements of the dielectric constants show that the PMN crystals do not undergo a sharp transition to a ferroelectric phase. Instead, the dielectric constant exhibits a broad maximum at $T_{\text{max}} \sim 270$ K.⁶ Below $T \sim 620$ K, the dielectric constant deviates from the Curie-Weiss law and exhibits strong frequency dispersion below 350 K.⁶ Relaxors also show x-ray and neutron diffuse scatterings⁷⁻⁹ along with broad Raman spectra. Brillouin scattering has been used to investigate the temperature dependencies of the longitudinal (L) and transverse (T) modes of PMN in backscattering geometry,^{10,11} which showed a minimum in the temperature dependence of the sound velocity near $T \sim 240$ K for L and T modes.

Knowledge of elastic, piezoelectric, and dielectric constants is fundamental for describing the electromechanical response of a material to applied strains and fields so a complete set of single-crystal tensor properties as a function of composition is desirable. Recently, a complete set of elastic and piezoelectric constants has been reported for multidomain and single domain $\text{Pb}(\text{Zn}_{1/3}\text{Nb}_{2/3})\text{O}_3-x\text{PbTiO}_3$ and PMN- x PT at several different compositions.¹²⁻¹⁶ High-pressure x-ray diffraction and Raman-scattering experiments revealed that PMN undergoes a structural change around 4 GPa at room temperature.^{7,8} In this paper, we study the elastic properties of single-crystal PMN under pressure and investigate above phase transition using micro-Brillouin scattering techniques.

Single crystals of PMN with cubic morphology were grown by the high-temperature solution technique.¹⁷ We have confirmed by x-ray analysis that the material has point-

group symmetry $m\bar{3}m$. A sample polished normal to the ab plane with a thickness of about 30 μm was loaded into a diamond-anvil cell (DAC). We used a 4:1 mixture of methanol and ethanol as the pressure medium. Neither birefringence nor domains were visible by polarized microscope before or after experiments, observations which are consistent with cubic symmetry.

A full description of the Brillouin scattering apparatus used in this study can be found elsewhere.¹⁸ A single-mode argon-ion laser ($\lambda = 514.5$ nm) was used as the excitation source with the average power less than 100 mW. The sample was placed symmetrically with respect to the incoming and collected light such that the difference vector of the two beams was in the plane of the sample. By rotating the sample around the $[001]$ direction, the scattering vector is rotated in the ab plane of the sample. The scattered light was analyzed by a 3+3 tandem Fabry-Perot interferometer, detected by a photon counting photomultiplier, and output to a multichannel scalar. Spectra were taken every 10° over half a full rotation of the sample and collected for an average of 2 h at each orientation.

Representative high-pressure Brillouin spectra of PMN are shown in Fig. 1. There are two pairs of peaks in each spectrum and an additional Rayleigh peak due to elastic scattering at zero frequency. One of the two pairs corresponds to the longitudinal-acoustic mode (L mode) and the other pair corresponds to the transverse-acoustic modes (T modes). Brillouin scattering due to the inelastic interaction of light with an acoustic phonon in the crystal results in a frequency shift $\Delta\nu$ of the incident light. The magnitude of the shift is related to the velocity of the acoustic phonon v propagating with the wave vector q , the refractive indices of the material, and the scattering angle θ . In these measurements, the sample was placed symmetrically with respect to the incoming and collected light. For this geometry, the frequency shift of the incident light is independent of the refractive index n of the sample (a detailed derivation can be found in Ref. 18). The Brillouin shifts $\Delta\nu_\theta$ are given by

$$\Delta\nu_\theta = (2v/\lambda)\sin(\theta/2), \quad (1)$$

where v is the sound velocity and λ is the incident wavelength.

The velocity of a plane acoustic wave propagating in a

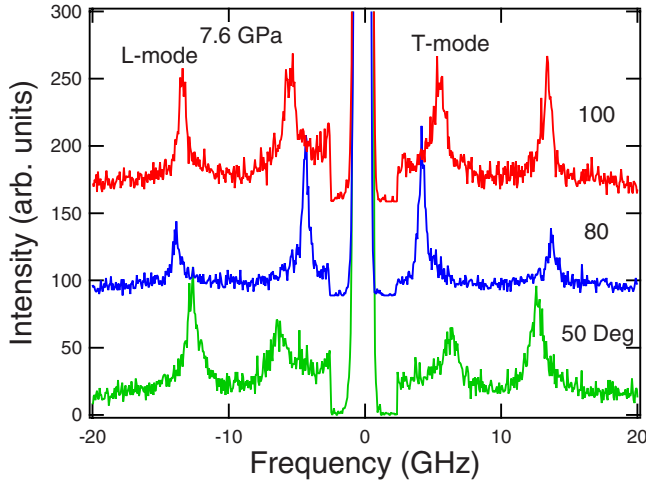


FIG. 1. (Color online) A typical set of Brillouin spectra at selected angles at 7.6 GPa. The longitudinal (*L*) and transverse (*T*) modes are clearly visible.

direction *q* is related to the elastic properties of the crystal via the Christoffel equation:

$$|\Gamma_{ik} - \delta_{ik}\rho v^2| = 0, \quad (2)$$

with

$$\Gamma_{ik} = \{C_{ijkl} + [(e_{mij}q_m)(e_{nkl}q_n)/(\epsilon_{rs}q_rq_s)]q_mq_n\}q_jq_l, \quad (3)$$

where δ_{ik} is the Kronecker delta with $\delta_{ik}=1$ for $i=k$ and $\delta_{ik}=0$ for $i \neq k$, and $\rho=8.12$ g/cm³, the density of PMN. C_{ijkl} , e_{mij} , and ϵ_{rs} are components of the elastic, piezoelectric stress, and dielectric permittivity tensors, respectively, and q_i are the directional cosines of the acoustic wave. There are four independent nonvanishing elastic constants for cubic (*m3m*) symmetry, which in Voigt matrix notation are C_{11} , C_{12} , C_{44} , and dielectric constant ϵ_{11} . There is no piezoelectric response in PMN and thus no contribution from the second part of Eq. (3) to the Brillouin shifts. Equation (2) is a cubic equation with three roots, ρv_i^2 , $i=1, 2, 3$, associated with one longitudinal and two transverse waves propagating in a given direction. The explicit expressions of Eq. (2) in the *ab* plane of a cubic crystal can be found in Ref. 15. The measured Brillouin shifts were inverted for a best-fit set of elastic constants by minimizing the sum of squares of residuals between the measured Brillouin shifts and those calculated from a trial set of constants using Eqs. (7)–(9) in Ref. 15 by the method described in Ref. 16. The nonlinear minimization procedure¹⁶ was used. The comparison of measured Brillouin shifts with those generated from our best-fit parameters is shown in Fig. 2. The fitted curves are in good agreement with the experimental data. The transverse mode related to C_{44} was not observed in measurements due to our experimental setup.^{15,16} It should be noted that we treated the PMN sample as a pseudocubic crystal between ambient and 10 GPa, and therefore there are only three elastic constants to be fitted.

Figure 3 shows the pressure dependencies of elastic constants C_{11} , C_{12} , and C_{44} obtained with a best fit at each pressure: C_{11} increases approximately linearly with pressure,

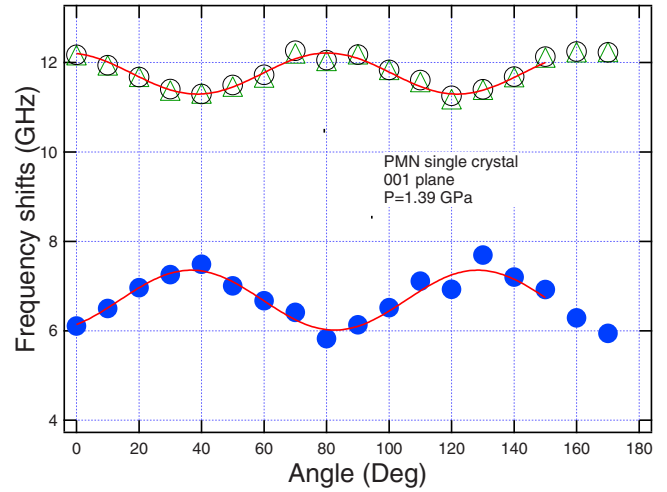


FIG. 2. (Color online) Plot of the experimental (marks) and model (lines) Brillouin shifts (GHz) of the longitudinal and transverse modes with angle for the *a-b* plane of the PMN crystal at 1.4 GPa.

whereas C_{12} exhibits a jump above 4.5 GPa, and C_{44} remains nearly constant. We also calculated the averaged elastic moduli such as the bulk modulus [$1/3(C_{11}+2C_{12})$] and shear modulus, with the shear modulus given in Voigt-Reuss-Hills¹⁹ terms (inset of Fig. 3). Figure 4 displays the pressure dependence of the elastic anisotropy: A

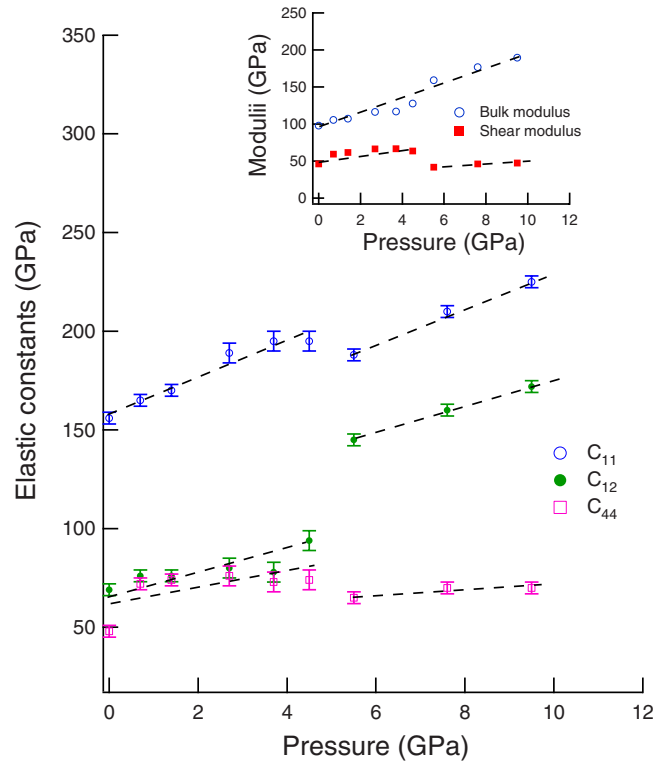


FIG. 3. (Color online) Pressure dependencies of the second-order elastic moduli. The marks are experimental data and dashed lines are guides to the eye. The inset shows the pressure dependencies of the bulk and shear moduli. The shear modulus was given as the Voigt-Reuss-Hills average.

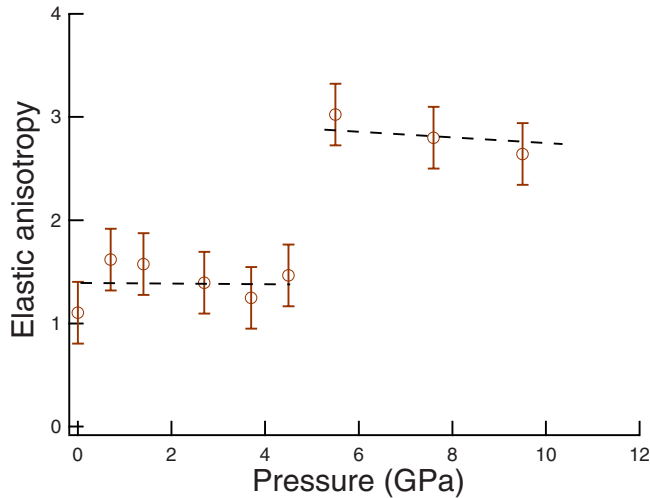


FIG. 4. (Color online) Pressure dependence of the elastic anisotropy of PMN. The marks are the data and the dashed line is a guide to the eye. It is obvious that there is an abrupt change in the elastic anisotropy of PMN at 4.5 GPa.

$=2C_{44}/(C_{11}-C_{12})$; A is about 1.7 below 4 GPa and 2.5 above 5 GPa, indicating a structural change above 4 GPa, consistent with previous high-pressure x-ray⁷ and Raman measurements.⁸ The error in the measurement of Brillouin shifts is less than 0.1 GHz, which introduces an error in the calculation of elastic modulus of less than 0.05 GPa. However, we obtained the elastic constants via fitting the angular dependence of the Brillouin shifts, and therefore the errors in the elastic constants are larger than 0.05 GPa. For example, we obtained $C_{11}=170 \pm 3$ GPa at 1.4 GPa.

We suggest that PMN undergoes a structural transforms from the cubic $Pm3m$ to rhombohedral $R3c$ structure at 4.5 GPa. First-principles calculations predict that the prototype ferroelectric lead titanate undergoes a series of structural phase transitions with increasing pressure according to the following sequence: $P4mm \rightarrow Cm \rightarrow R3m \rightarrow R3c \rightarrow R-3c$.²⁰ For other perovskite ferroelectrics, although the detailed phase-transition sequence will depend on the ground state and chemical composition, the computational results can be generalized as seen from the results for $PbZr_{0.52}Ti_{0.48}O_3$ (PZT).²¹ It has been proposed that PZT undergoes a phase transition under pressure according to the following se-

quence: $Cm \rightarrow R3m$ (2 GPa) $\rightarrow R3c$ (5 GPa) $\rightarrow R-3c$ (7 GPa) at 300 K.²¹ The proposed rhombohedral $R3c$ phases in PT and PZT under pressure have both polar distortions and antiphase oxygen octahedral rotations. The calculations, however, suggest that the $R3c$ structure in perovskite ferroelectric PT could have a nonpolar state with antiphase oxygen octahedral rotations and still be stable at high pressure.²⁰ Since PMN has an averaged cubic structure with rhombohedral ($R3m$) local distortions,²² the high-pressure phase of PMN could have the nonpolar $R3c$ structure.²³ Thus, the measured angular dependence of sound velocity will be in pseudocubic $a-b$ plane in $R3c$. The pseudocubic $a-b$ plane is very close to the original cubic $a-b$ plane, and the polarization properties or the acoustic modes would be very similar so that it is difficult to observe the third peak in the spectra (Fig. 1), (cf. Ref. 15). Additional evidence comes from high-pressure Raman-scattering measurements of PMN (Ref. 8) and PZT,²¹ which show a new sharp Raman band around 380 cm^{-1} under pressure. This band is attributed to an antiphase oxygen octahedral rotation in the rhombohedral $R3c$ structure.²¹ One explanation for such a change is that pressure suppresses the B -site displacement disorder of the perovskite structure; this can be seen from the disappearance of diffuse scattering with pressure.⁷ Consequently the local competition between A and B site displacements changes with pressure. It is therefore possible that pressure induces antiphase tilts of octahedra in the perovskite structure to balance the competition between A and B sites as observed in several materials such as PZT.²¹

The pressure dependencies of elastic constants of PMN single crystal have been derived from micro-Brillouin scattering spectroscopy. We also obtained the pressure dependence of the elastic anisotropy. The changes in elastic moduli and anisotropy at 4.5 GPa indicate that PMN single crystal undergoes a structural transition from a cubic $Pm3m$ to a rhombohedral $R3c$ phase at 4.5 GPa, a result that is in good agreement with the previous high-pressure x-ray and Raman studies.

We are grateful to S. Gramsch for comments on the manuscript and discussions. This work was sponsored by the Office of Naval Research under Grants No. N00014-02-1-0506, No. N00014-97-1-0052, and No. N00014-99-06-1-0166. Support also was received from the Carnegie/DOE Alliance Center (CDAC Contract No. DE-FC03-03NA00144) and National Science Foundation Grant No. DMR-0805056.

¹S. E. Park and T. R. Shrout, J. Appl. Phys. **82**, 1804 (1997).

²Z. G. Ye, Key Eng. Mater. **155-156**, 81 (1998).

³B. P. Burton, E. Cockayne, S. Tinte, and U. V. Waghmare, Phase Transitions **79**, 91 (2006).

⁴A. A. Bokov and Z. G. Ye, J. Mater. Sci. **41**, 31 (2006).

⁵N. de Mathan, E. Husson, G. Calvarn, J. R. Gavarri, A. W. Hewat, and A. Morell, J. Phys.: Condens. Matter **3**, 8159 (1991).

⁶V. Bovtun, S. Kamba, A. Pashkin, M. Savinov, P. Samoukhina, J. Petzelt, I. P. Bykov, and M. D. Glinchuk, Ferroelectrics **298**, 23

(2004).

⁷B. Chaabane, J. Kreisel, B. Dkhil, P. Bouvier, and M. Mezouar, Phys. Rev. Lett. **90**, 257601 (2003).

⁸J. Kreisel, B. Dkhil, P. Bouvier, and J. M. Kiat, Phys. Rev. B **65**, 172101 (2002).

⁹M. Ahart, R. E. Cohen, V. Struzhkin, E. Gregoryanz, D. Rytz, S. A. Prosandeev, H. K. Mao, and R. J. Hemley, Phys. Rev. B **71**, 144102 (2005).

¹⁰C. S. Tu, V. H. Schmidt, and I. G. Siny, J. Appl. Phys. **78**, 5665 (1995).

- ¹¹S. G. Lushnikov, J. H. Ko, and S. Kojima, *Appl. Phys. Lett.* **84**, 4798 (2004).
- ¹²R. Zhang, B. Jiang, and W. Cao, *Appl. Phys. Lett.* **82**, 787 (2003).
- ¹³R. Zhang, W. Jiang, B. Jiang, and W. Cao, (unpublished).
- ¹⁴J. Yin, B. Jiang, and W. Cao, *IEEE Trans. Ultrason. Ferroelectr. Freq. Control* **47**, 285 (2000).
- ¹⁵M. Ahart, A. Asthagiri, Z. G. Ye, P. Dera, H.-k. Mao, R. E. Cohen, and R. J. Hemley, *Phys. Rev. B* **75**, 144410 (2007).
- ¹⁶M. Ahart, A. Asthagiri, P. Dera, H. K. Mao, R. E. Cohen, and R. J. Hemley, *Appl. Phys. Lett.* **88**, 042908 (2006).
- ¹⁷Z. G. Ye, P. Tissot, and H. Schmid, *Mater. Res. Bull.* **25**, 739 (1990).
- ¹⁸C. S. Zha, R. J. Hemley, H. K. Mao, T. S. Duffy, and C. Meade, *Phys. Rev. B* **50**, 13105 (1994).
- ¹⁹Robert E. Newnham, *Properties of Materials* (Oxford University Press, New York, 2005), p. 114.
- ²⁰P. P. Ganesh and R. E. Cohen, *J. Phys.: Condens. Matter* **21**, 064225 (2009).
- ²¹A. Sani, B. Noheda, I. A. Kornev, L. Bellaiche, P. Bouvier, and J. Kreisel, *Phys. Rev. B* **69**, 020105(R) (2004).
- ²²W. Dmowski, S. B. Vakhrushev, I.-K. Jeong, M. P. Hehlen, F. Trouw, and T. Egami, *Phys. Rev. Lett.* **100**, 137602 (2008).
- ²³Raman scattering (Ref. 7) and x-ray diffraction (Ref. 8) measurements indicate a lowering of symmetry at this pressure, but these studies were unable to identify the symmetry unambiguously. Based on a parallel with other perovskite ferroelectrics, we therefore we expect this phase to have the $R3c$ structure. The crystallographic direction along which the reported measurements have been made cannot distinguish between a cubic and rhombohedral symmetry. These measurements were hence intended to point to the elastic origin of the transformation in PMN.